Journal of Animal Science, 2020, 1–10

doi:10.1093/jas/skaa044
Advance Access publication February 6, 2020
Received: 15 November 2019 and **Accepted:** 5 February 2020
Meat Science

MEAT SCIENCE

Mitochondrial oxygen consumption in early *postmortem* permeabilized skeletal muscle fibers is influenced by cattle breed

Patricia M. Ramos,[*,†] Chengcheng Li,[†] Mauricio A. Elzo,[†] Stephanie E. Wohlgemuth,[‡] and Tracy L. Scheffler[†,1]

[*]Department of Animal Sciences, "Luiz de Queiroz" College of Agriculture, University of Sao Paulo, 13418-900 Piracicaba, SP, Brazil, [†]Department of Animal Sciences, University of Florida, Gainesville, FL 32611, [‡]Department of Aging and Geriatric Research, University of Florida, Gainesville, FL 32603

[1]Corresponding author: tscheffler@ufl.edu

Abstract

Functional properties and integrity of skeletal muscle mitochondria (**mt**) during the early *postmortem* period may influence energy metabolism and pH decline, thereby impacting meat quality development. Angus typically produce more tender beef than Brahman, a *Bos indicus* breed known for heat tolerance. Thus, our objectives were to compare mt respiratory function in muscle collected early *postmortem* (1 h) from Angus and Brahman steers (n = 26); and to evaluate the effect of normal and elevated temperature on mt function ex vivo. We measured mt oxygen consumption rate (**OCR**) in fresh-permeabilized muscle fibers from Longissimus lumborum (**LL**) at 2 temperatures (38.5 and 40.0 °C) and determined citrate synthase (**CS**) activity and expression of several mt proteins. The main effects of breed, temperature, and their interaction were tested for mt respiration, and breed effect was tested for CS activity and protein expression. Breed, but not temperature ($P > 0.40$), influenced mt OCR (per tissue weight), with Brahman exhibiting greater complex I+II-mediated oxidative phosphorylation capacity ($P = 0.05$). Complex I- and complex II-mediated OCR also tended to be greater in Brahman ($P = 0.07$ and $P = 0.09$, respectively). Activity of CS was higher in LL from Brahman compared to Angus ($P = 0.05$). Expression of specific mt proteins did not differ between breeds, except for higher expression of adenosine triphosphate (**ATP**) synthase subunit 5 alpha in Brahman muscle ($P = 0.04$). Coupling control ratio differed between breeds ($P = 0.05$), revealing greater coupling between oxygen consumption and phosphorylation in Brahman. Our data demonstrate that both Angus and Brahman mt retained functional capacity and integrity 1-h *postmortem*; greater oxidative phosphorylation capacity and coupling in Brahman mt could be related to heat tolerance and impact early *postmortem* metabolism.

Key words: beef, *Bos indicus*, Brahman, mitochondria, oxygen, *postmortem* metabolism

Introduction

Traditionally, *postmortem* muscle metabolism has been viewed as an anaerobic process dependent on breakdown of glycogen to lactate and H^+. Although anaerobic glycolysis contributes significantly to adenosine triphosphate (**ATP**) production, there is growing evidence that mitochondrial (**mt**) respiratory activity affects *postmortem* metabolism and meat quality development. When muscle glycogen is not limiting, acidification is influenced by phosphofructokinase activity and mt content (England et al., 2014, 2018; Matarneh et al.,

Abbreviations

ADP	adenosine diphosphate
ATP	adenosine triphosphate
ATP5A	adenosine triphosphate synthase (complex V subunit alpha)
BIOPS	biopsy preservation medium
COX4	cytochrome *c* oxidase (complex IV subunit 4)
CS	citrate synthase
Cyt *c*	cytochrome *c*
ECII	maximum uncoupled respiration (succinate-supported)
ETS	electron transport system
FCCP	uncoupler carbonyl cyanide 4-(trifluoromethoxy) phenylhydrazone
LEAK or L	respiration after addition of NADH-linked substrates (glutamate, malate, pyruvate)
L_O	LEAK after oligomycin
LL	Longissimus lumborum
Mb	myoglobin
MiR05	mitochondria respiration medium
mt	mitochondria/mitochondrial
OCR	oxygen consumption rate
OXPHOS	oxidative phosphorylation
PCI	respiration after ADP
PCI+CII	respiration after succinate
PCII	respiration after rotenone (complex I inhibited)
ROX	residual oxygen consumption
SDHB	succinate dehydrogenase (complex II iron-sulfur protein subunit)
SUIT	substrate-uncoupler-inhibitor titration
TBS	Tris-buffered saline
VDAC	voltage-dependent anion channel (porin)

2017, 2018). In an in vitro model of *postmortem* metabolism with isolated mt, inhibition of mt complex activity resulted in more rapid ATP and pH decline (Scheffler et al., 2015). England et al. (2018) showed that electrical stimulation of bovine Longissimus lumborum (**LL**) *postmortem* hastens the decline in oxygenation compared to nonstimulated muscle; this was linked to more rapid glycogen and ATP disappearance, faster pH decline, and compromised mt function. This suggests that mt in muscle retain the capacity to produce ATP aerobically for some time post-exsanguination; thus, mt likely play a role in determining cellular conditions and meat quality development.

Mitochondrial capacity for ATP production in vivo depends on both quantitative and qualitative properties. These mt properties are related not only to muscle fiber type and mt subcellular location, but also the animal's genetics, physiology, and environment. For example, compared to fast fibers, slow fibers exhibit greater mt density which contributes markedly to oxidative ATP production; however, genetics, diet, and physical activity, among other factors, affect mt density in a muscle (Granlund et al., 2011; Egan and Zierath, 2013; Liu et al., 2016; Apaoblaza et al., 2020). Qualitative mt attributes, such as surface area:volume, membrane fluidity (phospholipid composition), and cristae surface area, may specialize mt to meet specific functional demands according to fiber type and subcellular location (subsarcolemmal or intermyofibrillar) (Picard et al., 2012) or modulate respiratory function (Heden et al., 2016). Various conditions in humans, such as aging, resistance exercise, and mild repeated heat stress (Porter et al., 2015a, 2015b; Hafen et al., 2018), can alter mt respiratory function independently of mt content. Hence, it is possible that mt properties also contribute to variation in *postmortem* muscle energy metabolism.

Recently, we demonstrated that citrate synthase (**CS**) activity, a marker of mt content, was positively correlated with the proportion of Brahman influence in an Angus–Brahman multibreed herd (Wright et al., 2018). The increased heat tolerance seen in the Brahman breed could be associated with elevated mt content, and possibly with mt functional properties that facilitate the animal's physiology at higher temperatures. Temperature and climate influence metabolism, and variation in mt function likely contributes to adaptation and whole-animal thermal tolerance (James and Tallis, 2019; Milani and Ghiselli, 2020). Specifically, tighter coupling between mt proton pumping and ATP synthesis means that more ATP is produced and less heat dissipated. Therefore, lower heat production and greater heat tolerance in Brahman could be a consequence of increased mt efficiency. Greater efficiency of mt ATP production would also be consistent with slower pH decline and ATP disappearance *postmortem* in LL of Brahman compared to Angus (Ramos et al., 2020). Thus, we anticipated that subspecies (*Bos taurus* vs. *Bos indicus*) and temperature affect mt function in early *postmortem* LL. Therefore, our objectives were to assess mt respiratory function in permeabilized muscle fibers collected early *postmortem* (1 h) from Brahman- and Angus-influenced cattle; and to evaluate the effect of physiological (38.5 °C) and elevated (40 °C) temperatures on mt function. We hypothesized that mt oxygen consumption rate (**OCR**) in LL muscle fibers is higher in Brahman compared to Angus, and that mt respiration would remain higher in Brahman at elevated temperature in agreement with this breed's heat tolerance.

Materials and methods

Animals and sampling

The animals used in this study are part of a long-term genetic evaluation program conducted at the University of Florida. Procedures were approved by the Institutional Animal Care and Use Committee (IACUC #201503744). All animals were under the same husbandry during growing and fattening phases. Only animals classified as Angus or Brahman were used for this study (genetic composition varying from 100% to 80%; Elzo et al., 2012), with a final average live weight and age of 577.3 ± 70.6 kg and 18.7 ± 1.23 mo, respectively. The day before slaughter, animals were transported in the morning for approximately 55 km on pavement road to Gainesville, FL, and stayed in lairage with free access to water. The slaughter occurred in the Meat Processing Center at the University of Florida, under inspection by the United States Department of Agriculture (USDA-FSIS). Slaughter occurred during summer in 2 consecutive years, with 3 dates per summer. On each day, 2 animals from each breed were sampled, except the last day when 3 animals were sampled (n = 26; 13 per breed). Approximately 1-h *postmortem* (40 min to 1 h) samples from LL were collected and either stored in ice-cold (0 °C) biopsy preservation medium (**BIOPS**; 2.77 mM CaK_2EGTA, 7.23 mM K_2EGTA, 5.77 mM Na_2ATP, 6.56 mM $MgCl_2 \cdot 6H_2O$, 20 mM taurine, 15 mM Na_2phosphocreatine, 20 mM imidazole, 0.5 mM dithiothreitol, and 50 mM MES; pH 7.1; Saks et al., 1998) for immediate respirometry analysis, or frozen in liquid nitrogen and kept in an ultra-low temperature freezer (–80 °C) until electrophoresis and enzyme activity analyses were conducted.

High-resolution respirometry

Tissue permeabilization

Respirometry was conducted with fresh muscle samples (40-min to 1-h *postmortem*) within 5 h of collection. Samples were cleaned of visual fat and connective tissue. Using a dissection microscope, a bundle of muscle fibers was selected and cleaned once more from residual fat and connective tissue using a pair of forceps, followed by a delicate procedure of fiber teasing as previously described in more detail by Kuznetsov et al. (2008). For fiber permeabilization, approximately 2 to 4 mg of tissue was transferred to a microtube containing saponin solution (50 µg/mL in BIOPS) and incubated for 20 min at 4 °C on a rotator (Kuznetsov et al., 2008). The bundle was rinsed in ice-cold mt respiration medium (**MiR05**; 0.5 mM EGTA, 3 mM $MgCl_2 \cdot 6H_2O$, 60 mM lactobionic acid, 20 mM taurine, 10 mM KH_2PO_4, 20 mM HEPES, 110 mM d-sucrose, and 1 g/L BSA essentially fatty acid free, pH 7.1; Fasching et al., 2016), and washed in MiR05 for 10 min at 4 °C before the bundle was carefully blotted dry and wet weight (mg) determined. Mitochondrial respiration of those samples was immediately assessed using high-resolution respirometry.

High-resolution respirometry

Several Oroboros O2k (Oroboros Instruments, Innsbruck, Austria) respirometers were used, and calibrated by a 2-point calibration (air saturation and zero-oxygen) immediately prior to an experiment with MiR05 at the experimental temperature (38.5 and 40.0 °C, respectively). Additionally, instrumental background oxygen flux was determined at the respective experimental temperature for each instrument and sensor used, and the acquired data corrected accordingly by the acquisition and analysis software (DatLab vs 7.0, Oroboros Instruments). Mitochondrial respiration of permeabilized fibers (2 to 4 mg wet weight) was determined in duplicate at the desired experimental temperature. The respiration medium MiR05 was supplemented with 20 mM creatine to saturate mt creatine kinase, which facilitates adenosine diphosphate (**ADP**) transport (Walsh et al., 2001), and measurements were conducted under hyperoxic conditions (250 to 450 µM O_2) as previously described by Li et al. (2016). Integrative OCR (ρmol/s/mg tissue) was determined using the following substrate-uncoupler-inhibitor titration (**SUIT**) protocol (Fig. 1; concentration of reagents noted in parentheses are final concentrations in the respirometer chamber): 1) addition of NADH-linked substrates glutamate (10 mM), malate (2 mM), and pyruvate (5 mM) to support electron flow through complex I (CI) of the electron transport system (**ETS**), recorded as **LEAK** respiration (L); 2) addition of ADP (2.5 mM) to stimulate respiration and oxidative phosphorylation (**OXPHOS**, $\mathbf{P}_{CI}$); 3) addition of succinate (10 mM) to support convergent electron flow to complexes I and II of the ETS (OXPHOS, $\mathbf{P}_{CI+II}$); 4) addition of cytochrome *c* (**cyt c**, 10 µM) to test mt outer membrane integrity (permeabilization quality control; samples with an increase of respiration of more than 15% after cyt *c* addition were removed from the analysis); 5) addition of rotenone (0.5 µM) to inhibit complex I (OXPHOS, $\mathbf{P}_{CII}$); 6) addition of oligomycin (5 nM) to inhibit ATP synthase, recorded as LEAK respiration in the presence of oligomycin (L_O); 7) step-wise addition of the uncoupler carbonyl cyanide 4-(trifluoromethoxy) phenylhydrazone (**FCCP**, 0.5 µL steps of a 0.1 mM stock solution) to reach maximum uncoupled respiration, recorded as succinate-supported ETS capacity ($\mathbf{E}_{CII}$); 8) addition of antimycin A (2.5 µM) to inhibit complex III of the ETS and thereby OXPHOS, recorded as residual oxygen consumption (**ROX**), which represents non-mt OCR and was subtracted from all OCRs at the preceding respiratory states. The coupling efficiency was calculated as $1 - (L/P_{CI})$, as well as coupling control, calculated as L/P_{CI+II}, and the OXPHOS control ratio as P_{CII}/E_{CII}.

Citrate synthase activity

For CS activity, a subsample of the frozen muscle was pulverized in liquid nitrogen, homogenized as described below, and enzyme activity immediately measured. Pulverized muscle (approximately 50 mg) was diluted 1:20 (w/v) using ice-cold extraction buffer (0.25 M sucrose, 1 mM EDTA, 10 mM Tris-Cl, pH 7.4). Homogenization was performed at 5,000 rpm for 10 s with a bead homogenizer (Precellys 24, Bertin Instruments, Hialeah, FL), followed by brief sonication (15× 1 s; 60 Sonic Dismembator, Fisher Scientific, Hampton, NH). Enzyme activity was measured with a multi-well plate reader (Synergy HT, BioTek Instruments, Winooski, VT) set to 37 °C, and following procedures described by Wright et al. (2018). A linear change in absorbance for an interval

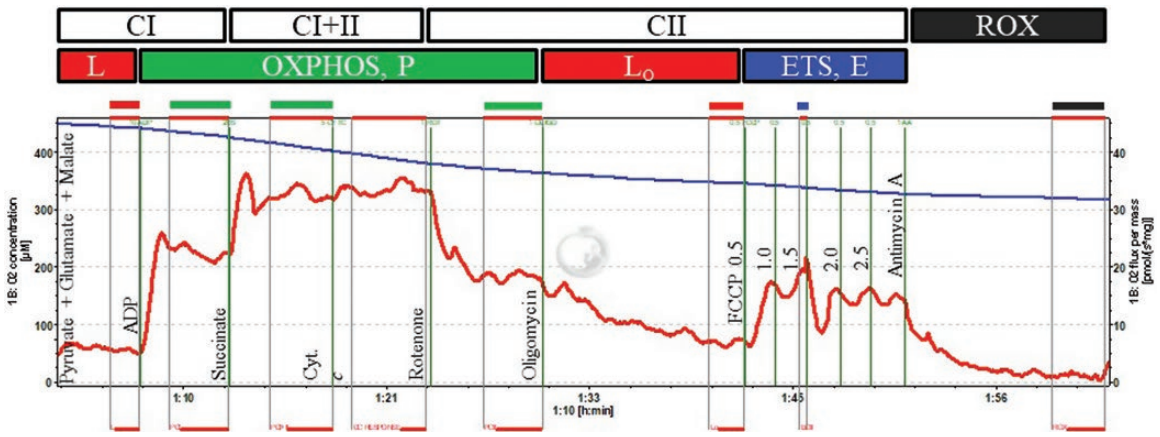

Figure 1. Respirometry protocol and example trace using permeabilized fibers from Angus or Brahman Longissimus lumborum muscle at 1-h *postmortem*. Oxygen flux per mass (ρmol/s/mg tissue; red line), and oxygen concentration (nmol/mL; blue line). The following SUIT protocol was performed: 1) malate, glutamate, pyruvate (2, 10, and 5 Mm, respectively; LEAK respiration, L); 2) ADP (2.5 mM; activated respiration, P_{CI}); 3) succinate (10 mM; activated respiration, P_{CI+II}), 4) cytochrome *c* (10 µM; quality control; see text for details); 5) rotenone (0.5 µM; activated respiration after inhibition of complex I, P_{CII}); 6) oligomycin (5 nM; LEAK respiration induced by oligomycin-induced inhibition of ATP synthase; L_O); 7) carbonyl cyanide 4-(trifluoromethoxy) phenylhydrazone (FCCP, 0.05 µM steps; maximum succinate-supported electron transport capacity, E_{CII}); 8) antimycin A (2.5 µM; residual oxygen consumption, ROX).

of 4 min was selected to calculate CS activity (ΔA412 nm = $A_{4\,min} - A_{0\,min}$). For final calculation of enzyme activity (nmol/min/mg tissue), initial weight (mg), extinction coefficient of 5-thio-2-nitrobenzoic acid (13.6 mM), dilution factor, and specific volumes were used.

Protein expression

Mitochondrial proteins were extracted by diluting pulverized samples 1:10 (w/v) with extraction buffer (50 mM Tris-base; 1 mM EDTA, pH adjusted at cold to 7.5); supplemented with 10% glycerol, 1% Triton-X, 50 mM sodium fluoride, 1 mM dithiothreitol, and 5 µL/mL protease inhibitor cocktail (Sigma, St. Louis, MO). Samples were homogenized once at 5,000 rpm for 10 s with a bead homogenizer (Precellys 24 Homogenizer; Bertin Instruments, Hialeah, FL), followed by sonication (10× 1 s), and incubation on ice for 20 min (Wadley and McConell, 2007). Samples were subsequently centrifuged at 10,000 × *g* for 20 min at 4 °C, and the supernatant collected. Protein concentration was determined using a Pierce protein assay with ionic detergent compatibility reagent (Thermo Scientific, Rockford, IL). Supernatants were diluted with buffer and 5× Laemmli buffer (0.5 M Tris-base, pH 6.8, 0.5 M dithiothreitol, 10% SDS, 0.5% bromophenol blue, and 50% glycerol) to achieve equal protein concentrations. Final samples were heated at 95 °C for 5 min and stored at –20 °C.

Proteins were separated by SDS–polyacrylamide gel electrophoresis (MGV-202-20, C.B.S. Scientific, San Diego, CA), using 10% (CS and voltage-dependent anion channel, **VDAC**) and 15% (other proteins: myoglobin, **Mb**; succinate dehydrogenase iron-sulfur subunit, **SDHB**; cyt *c*; cytochrome *c* oxidase or complex IV subunit 4, **COX4**; and ATP synthase subunit alpha, **ATP5A**) polyacrylamide resolving gels. Wells were loaded with equal amounts of protein (5 µg for CS and Mb, 10 µg for VDAC, and 15 µg for cytochrome *c* oxidase, ATP5A, SDHB, and cyt *c*), and the electrophoresis performed in running buffer (25 mM Tris-base, 0.2 M glycine, and 0.1% SDS) at 60 V for 20 min followed by additional running at 125 V determined according to protein size. Proteins were transferred to a nitrocellulose membrane (Thermo Scientific, Rockford, IL) using wet tank transfer (EBU 402, CBS Scientific, San Diego, CA) at 500 mA, 4 °C for 1 h with cold transfer buffer (50 mM Tris-base, 0.38 M glycine, 0.01% SDS, and 10% methanol). Subsequently, the membranes were dried overnight.

Total protein stain (REVERT, LI-COR, Lincoln, NE) was used to validate equal loading and to normalize the specific protein signal. Membranes were scanned using Odyssey CLx (LI-COR, Lincoln, NE), and a range of bands per lane were quantified using Image Studio software version 5.2. After protein staining, the membranes were washed in 1× Tris-buffered saline (**TBS**), pH 7.6, for 2 min then blocked with Starting Block (TBS) Blocking Buffer (Thermo Scientific, Rockford, IL) for 1 h. Primary antibodies were diluted 1:1,000 in blocking buffer with 0.2% Tween 20. The following primary antibodies were used: anti-CS (ab96600, Abcam, Cambridge, MA); anti-VDAC (#4866, Cell Signaling, Danvers, MA); anti-Mb (ab231530, Abcam, Cambridge, MA); anti-SDHB (ab14714, Abcam, Cambridge, MA); anti-cyt *c* (ab110325; Abcam, Cambridge, MA); anti-COX4 (#4850, Cell Signaling, Danvers, MA); and anti-ATP5A (ab14748, Abcam, Cambridge, MA). Membranes were incubated with primary antibody overnight at 4 °C on a rotator. The next day, membranes were washed 4 times with 1× TBS with 0.1% Tween 20 for 5 min and incubated for 1 h in secondary antibody conjugated with fluorescent dye (IRDye 800CW, LI-COR, Lincoln, NE), diluted 1:10,000 in blocking buffer with 0.2% Tween 20. Finally, membranes were washed 4 times with 1× TBS-0.1% Tween 20 for 5 min each, followed by an additional wash with 1× TBS, pH 7.6, to remove Tween 20. Membranes were then scanned and quantified as described for total protein stain. The signal for the target protein band was normalized to protein content range of the lane representing the sample.

Statistical analysis

Data were analyzed as a complete randomized block design, with block being the slaughter day; the fixed effect of breed (Angus and Brahman) and temperature (38.5 and 40 °C) as well as their interaction were investigated using the mixed procedure from SAS (SAS University Studio, SAS Institute, Inc., Cary, NC). Temperature was considered as repeated measure and animal within slaughter day and breed was considered as random effect. Due to increased cyt *c* response (quality control with threshold previously established at 15%), 1 sample from Brahman at 38.5 °C was removed from the data set. For protein expression and enzyme activity data, temperature and interaction were removed from the model. Normal distribution of residuals and homogeneity of variance were tested for each parameter, and data transformation was applied when needed (L_O). Data were analyzed using alpha as 0.05, and *P*-values between 0.05 and 0.1 were considered as tendency or trend. Significance values for the fixed effects are presented as well as significant least-square means contrasts. Results are expressed as least-square means ± SE.

Results and Discussion

We measured mt respiratory function in LL muscle fibers collected 1 h after exsanguination to address the possibility that mt affect *postmortem* metabolism in Brahman and Angus muscle differently. The preparation of permeabilized muscle fibers instead of organelle isolation allows for in situ assessment of the entire mt population within a tissue sample, independent of size, network, location, or functional status, avoiding potentially selective isolation of specific mt subpopulations. High-resolution respirometry further allowed us to assess the contribution of specific ETS complexes or combinations of complexes by following a specific SUIT protocol. Finally, the titration of cyt *c* was used as a quality control step to evaluate the integrity of the outer mt membrane after sample processing (Kuznetsov et al., 2008). We applied a threshold of 15% increase in OCR following the addition of cyt *c* as indicator of compromised integrity. With the exception of 1 sample from Brahman submitted at 38.5 °C (which was subsequently excluded from further analysis), the cyt *c* response was below 15%, indicating that the outer membrane was conserved 1-h *postmortem*; and confirming that the permeabilization protocol used in our study was successful at evaluating mt respiration while preserving the characteristics and function of the mt ex vivo (Kuznetsov et al., 2008).

We conducted mt analyses at 38.5 and 40 °C to evaluate the impact of temperature on mt function in 2 bovine subspecies that differ in heat tolerance. Under low temperature-humidity index conditions, both Angus and Brahman exhibit rectal or vaginal temperatures near 38.5 °C; however, during high temperature-humidity conditions, temperatures in Angus may increase to 40 °C while temperature of Brahman increases to a lesser extent (~39.0 °C) (Dikmen et al., 2018; Sarlo Davila et al., 2019). These temperatures (38.5 and 40°C) also encompass diurnal variation in vaginal temperature in Angus cows on pasture during high temperature-humidity index conditions (Dikmen et al., 2018). In comparison, experimental conditions with

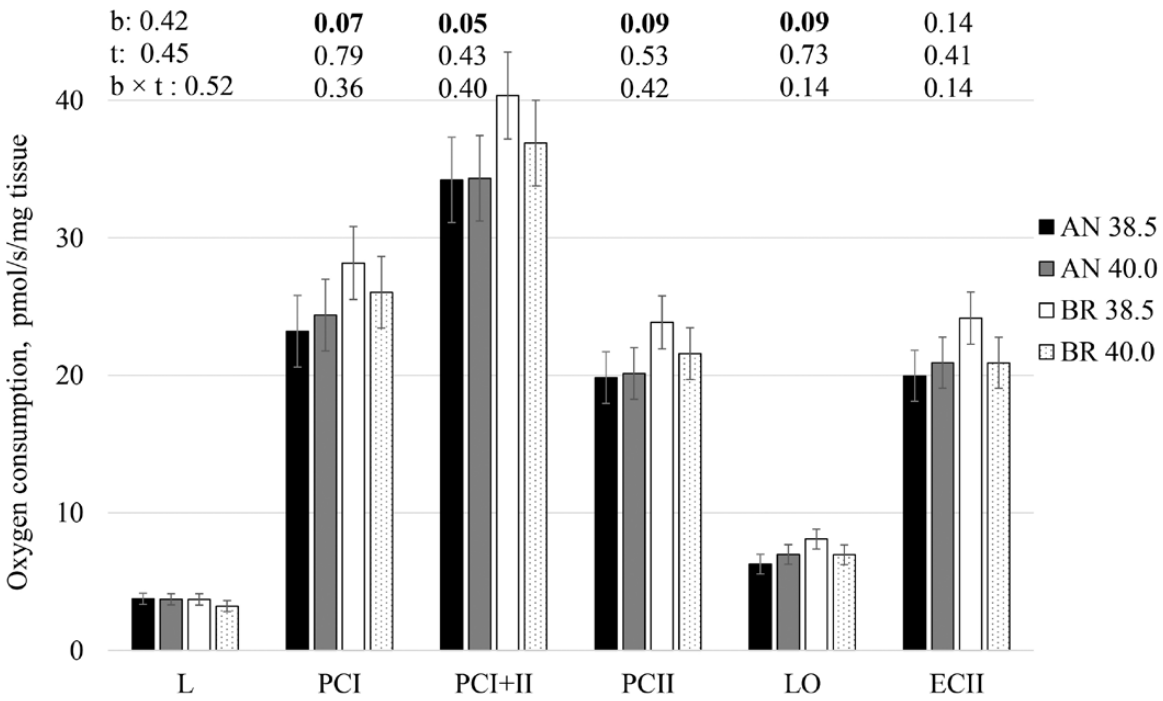

Figure 2. Integrative mitochondrial oxygen consumption rate (ρmol/s/mg tissue) of saponin-permeabilized Longissimus lumborum muscle fibers from Angus (AN) and Brahman (BR) at 1-h *postmortem* and 2 temperatures (38.5 and 40.0 °C). L: LEAK respiration in the presence of pyruvate, malate, and glutamate; PCI: activated respiration after addition of ADP; PCI+II: activated respiration after addition of succinate; PCII: activated respiration after inhibition of complex I; L_O: LEAK respiration after addition of oligomycin; ECII: succinate-supported maximum electron transport system capacity. See text for additional detail. Significance (*P*-value) for fixed effect of breed (*b*), temperature (*t*) and breed × temperature (*b* × *t*) for each parameter were presented (inset above each step). Bars represents least-square means followed by standard error.

prolonged, continuous heat and humidity resulted in maximum core temperatures greater than 40 °C for both Angus cross and Brahman heifers (41.2 and 40.4 °C, respectively), but remarkably, heifers still exhibited diurnal variation in core temperature (mean daily core temperature: 38.4 to 41.0 °C in Angus cross and 38.5 to 39.9 °C in Brahman) (Beatty et al., 2006). Therefore, Angus are more likely to reach 40 °C under normal pasture conditions, and Brahman are more resilient to environmental heat stress, even in extreme situations. Temperatures for mt analyses are also similar to reported temperatures of bovine LL at 1-h *postmortem* (typically between 37 and 39 °C), although *postmortem* temperature also depends on environmental temperatures *antemortem*, electrical stimulation, carcass mass, subcutaneous fat thickness, etc. (Jeremiah et al., 1985; Stolowski et al., 2006).

Integrative mt function

We found that integrative mt LEAK respiration (L) was similar between breeds and temperatures (Fig. 2). Upon addition of ADP, activated respiration with complex I-supporting substrates (P_{CI}), increased 7-fold in all conditions tested, and the corresponding coupling efficiency ($1 - L/P_{CI}$) ranged from 0.83 to 0.87, evidencing that mt were still capable of efficient OXPHOS 1-h *postmortem*. Independently of temperature, Brahman LL mt tended to consume more oxygen at P_{CI} compared to Angus (breed effect: $P = 0.07$). Convergent electron flow through both complex I and II caused an additional increase in OCR (P_{CI+II}), and Brahman showed greater OXPHOS capacity (P_{CI+II}) when compared to Angus (breed effect: $P = 0.05$). At this step (P_{CI+II}), a contrast revealed that at physiological temperature (38.5 °C) Brahman tended to consume more oxygen compared to Angus ($P = 0.06$). Breed tended to influence complex II activity (P_{CII}; $P = 0.09$), and again, at 38.5 °C Brahman tended to differ from Angus ($P = 0.08$).

Oligomycin blocks the proton channel (F_O domain) of ATP synthase, which inhibits both ATP synthesis and hydrolysis (Penefsky, 1985). Thus, OCR in the presence of oligomycin (L_O) is governed primarily by H^+ leak across the inner membrane and is expected to be similar to LEAK respiration in the presence of substrates but absence of ADP (L). Absolute values for L_O were higher than L, which could be due to hyperpolarization of the mt following inhibition of the ATP synthase and consequential exaggeration of the actual, voltage-dependent, proton leak (Divakaruni and Brand, 2011; Connolly et al., 2018). LEAK respiration in the presence of oligomycin tended to be influenced by breed ($P = 0.09$); similar to previous data, at 38.5 °C Brahman differed from Angus ($P = 0.03$).

Addition of an uncoupler increases proton conductance across the inner mt membrane, thereby allowing determination of maximum capacity of the ETS with a given supply of substrates, and in our SUIT protocol, this was succinate (E_{CII}; Fig. 2). At this step, mt OCR was not influenced by breed or temperature, but interestingly, the contrast revealed that mt OCR in LL from Brahman at 38.5 °C was higher than Angus at same temperature ($P = 0.04$). Maximum ETS capacity (E_{CII}) did not exceed OXPHOS capacity (P_{CII}) in the presence of succinate in any of the samples and treatments. It is possible that the overestimation of L_O discussed above masked an excess capacity in bovine LL muscle. An underestimation of the ETS excess capacity due to preceding oligomycin addition has previously been reported in intact and cultured cells (Ruas et al., 2016). This result is important to consider in future investigations when evaluation of excess capacity is desired.

Citrate synthase activity and mt protein expression

In general, integrative OCR from Brahman LL were numerically higher than Angus. While increased OCR may be due to inherent differences between mt of the different breeds, it could also be due to differences in mt content. Therefore, we investigated mt content by determining CS activity, which is commonly used as a marker for mt content (Larsen et al., 2012). Citrate synthase activity in LL was greater ($P = 0.05$) in Brahman compared to Angus (Fig. 3), which is consistent with our previous study (Wright et al., 2018). We evaluated protein expression of CS and VDAC (porin) as additional indicators of mt content. To confirm that protein extraction, sample processing, and gel loading were similar between the breeds, the immunoblot membrane was stained for total protein, and this signal was used as a normalization index (Fig. 4A). Protein expression of VDAC and of CS were not different between breeds ($P = 0.17$ and 0.75, respectively; Fig. 4B and C). Differences in mt enzyme activity without differences in mt protein expression were reported by Fritzen et al. (2019), who demonstrated that endurance training in human skeletal muscle increases CS activity independent of other markers of mt content (mtDNA copy number, and expression of porin and cardiolipin). Endurance training in humans also increases volume density of mt, which is positively related to CS activity (Lundby et al., 2018). Mitochondria morphology and volume may differ among breeds, but that was beyond our scope for this study.

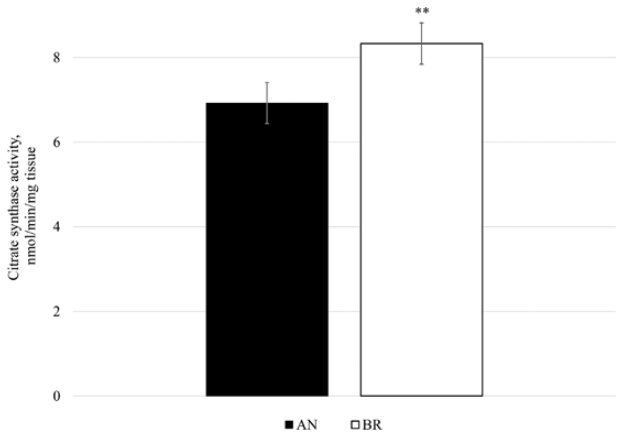

Figure 3. Citrate synthase activity (nmol/min/mg tissue) in Longissimus lumborum at 1-h *postmortem* from Angus and Brahman. **$P = 0.05$.

We tested expression of additional mt proteins in order to confirm that mt content between breeds was similar. In agreement with our findings for CS and VDAC, expression of SDHB, cyt *c*, and COX4 were similar between breeds ($P = 0.46$, $P = 0.98$, $P = 0.60$, respectively; Fig. 4B and C). However, ATP5A expression was 8% higher ($P = 0.04$) in Brahman compared to Angus LL. We anticipated that ATP5A may be related to activated respiration but did not find a significant correlation between P_{CI+II} and ATP5A expression ($P = 0.29$). Therefore, overall trends for higher OCR in Brahman appear to be related primarily to higher activity of ETS enzymes and not increases in protein expression of mt complexes.

Mitochondrial function may contribute to variation in *postmortem* metabolism and meat quality development. England et al. (2018) showed that decline in muscle oxygenation *postmortem* may be related to mt activity. One possible mechanism to sustain mt ATP production longer *postmortem* is greater Mb expression, which would increase oxygen storage capacity. In turn, greater supply of oxygen in *postmortem* muscle could enhance or extend the ATP-producing capacity of mt, thereby delaying pH decline. To address this possibility, we tested Mb expression and determined it was not different between Angus and Brahman LL mt ($P = 0.41$;

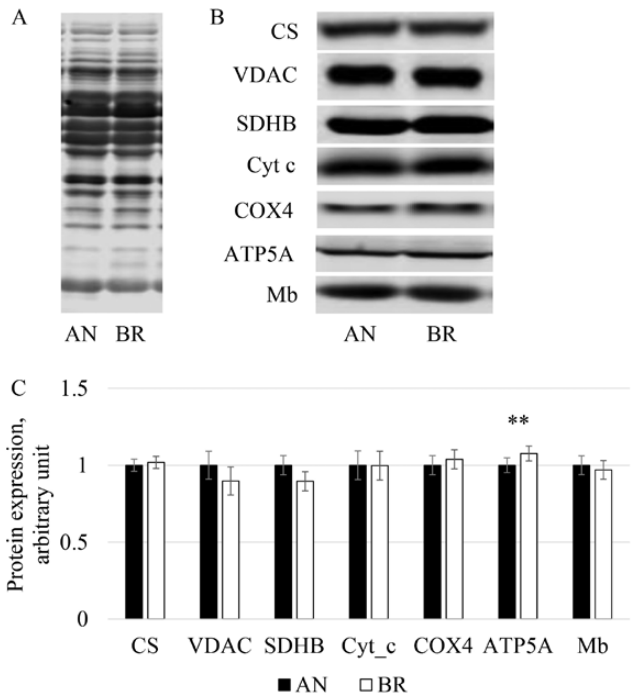

Figure 4. Mitochondrial protein content in Longissimus lumborum from Angus and Brahman. (A) Total protein stain; (B) immunodetection, and (C) content of CS = citrate synthase, VDAC = voltage dependent anion channel, SDHB = succinate dehydrogenase iron-sulfur protein subunit, Cyt_c = cytochrome c, COX4 = cytochrome c oxidase or IV subunit 4, ATP5A = ATP synthase or complex V subunit alpha, and Mb = myoglobin. **$P = 0.04$.

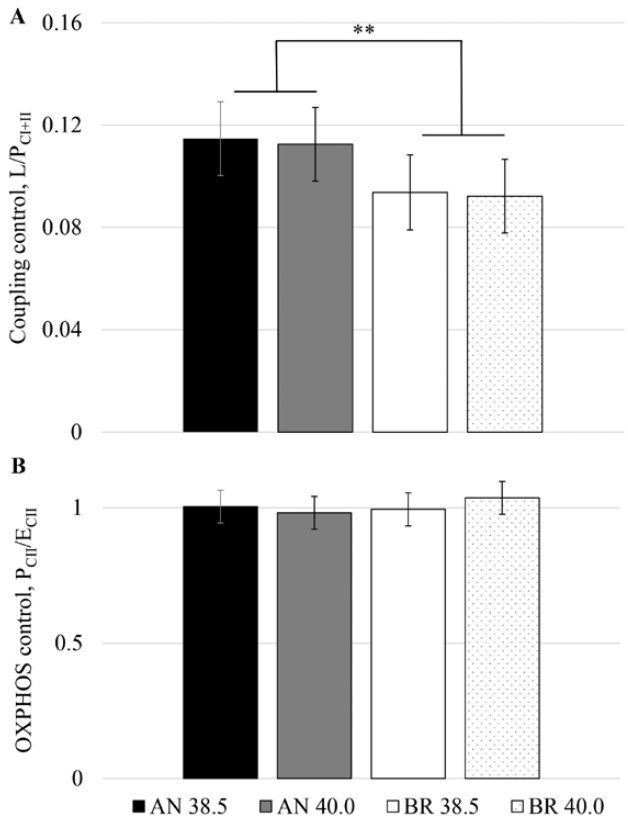

Figure 5. Mitochondrial coupling control ratios of permeabilized Longissimus lumborum at 1-h *postmortem* from Angus and Brahman at 2 temperatures (38.5 and 40.0 °C). (A) Coupling control L/P_{CI+II} (LEAK/OXPHOS; P_{CI+II}) and (B) OXPHOS control (P_{CII}/E_{CII}). **P = 0.05.

Fig. 4B and C). This reinforces that mt functional properties, revealed by overall higher OCR, CS activity, and expression of ATP5A in Brahman LL, may be contributing to the variation in *postmortem* metabolism of Brahman LL when compared to Angus, but these properties are not related to oxygen supply.

Coupling control ratios

We investigated the coupling control ratio ($LEAK/P_{CI+II}$) as an indicator for coupling of mt oxygen consumption and phosphorylation, and the limitation of the phosphorylation system. This ratio ranged from 0.09 to 0.11 (Fig. 5A), supporting that mt from both breeds were well-coupled at 1-h *postmortem*. Skeletal muscle obtained by biopsies from young and old quarter horses ranged from 0.06 to 0.10, with aging associated with a decrease in coupling efficiency (Li et al., 2016). Mitochondria from Brahman LL showed a lower and more favorable coupling control ratio than Angus (breed effect: $P = 0.05$), which was due to greater P_{CI+II} in Brahman (breed: $P = 0.05$). Therefore, substrate oxidation and oxygen consumption were more tightly coupled to energy production (phosphorylation) in mt from Brahman LL compared to Angus, independently of temperature.

The OXPHOS control ratio P_{CII}/E_{CII} did not differ between breeds ($P = 0.56$) and temperatures (Fig. 5B). In the noncoupled state after addition of FCCP (E_{CII}), the phosphorylation system (ATP synthase) is bypassed and electron flow and oxygen consumption are no longer coupled to ATP synthesis. Any previous limitations by the phosphorylation system would be apparent in an increase in OCR. The observed values (average = 1.00 ± 0.05) suggest that OXPHOS capacity with complex II-supporting substrate (P_{CII}) was not limited by the phosphorylation system. However, as mentioned before, the overestimation of LEAK (L_O) in oligomycin-treated skeletal muscle sample could have led to an underestimation of the apparent excess capacity (Ruas et al., 2016). The OXPHOS capacity in equine skeletal muscle was limited by the phosphorylation system to between 75% (Li et al., 2016) and 85% (Votion et al., 2012). Further studies will have to examine the degree of control of the OXPHOS system by the phosphorylation system in bovine LL muscle mt in the presence of convergent electron flow (P_{CI+II}/E_{CI+II}), which our SUIT protocol did not allow.

The basis for increased P_{CI+II} and coupling efficiency in Brahman LL is not clear, but could be related to homeostatic adjustments initiated either *antemortem* or *postmortem*, or both. Changes in mt function may involve membrane composition, including that of mt membranes. Membrane fluidity can affect protein diffusion. It also changes with temperature and lipid composition, and thus heat stress can affect membrane potential, alter intracellular ion levels (Balogh et al., 2011) and possibly cause increased proton conductance of the inner mt membrane. In livestock, environmental heat stress increased free radical production and lipid peroxidation, leading to downregulation of cellular energy production and reduced animal performance (Slimen et al., 2016). However, whether these findings were associated with altered mt membrane composition has not been investigated. Interestingly, in rats, membrane composition of subsarcolemmal mt was different between muscles, with more glycolytic plantaris muscle showing an increase in unsaturation index compared to more oxidative soleus muscle (Stefanyk et al., 2010); this is potentially linked to a more fluid membrane that facilitates reactive oxygen species-mediated regulation of proton leak during different states of energy demand (rest vs. exercise). Considering that we found differences in coupling control ratio between the breeds it seems possible that different mt membrane composition or mt subpopulation profile is underlying this diverse physiological response. However, a more in-depth characterization and comparison of mt subpopulations in skeletal muscle in these breeds is necessary to link mt morphology with heat tolerance in cattle breeds. Alternatively, greater P_{CI+II} and coupling efficiency in Brahman LL may be related to breed-specific responses to environmental heat and humidity prior to harvest. Cattle were exposed to environmental conditions typical for Florida summer, so Angus steers were more likely to have experienced heat stress compared to Brahman. Thus, lower P_{CI+II} and coupling efficiency in Angus LL may be the consequence of aforementioned increase in oxidative stress and downregulation of cellular energy production linked to heat stress. This is consistent with mt function differences between breeds yet similar mt protein content. Along these lines, in oxidative skeletal muscle of pigs, heat stress contributed to suppression of mitophagy and allowed dysfunctional mt to remain in the cellular environment (Brownstein et al., 2017). On the other hand, repeated exposure to mild heat stress in humans elicited positive adaptations on mt respiratory capacity (Hafen et al., 2018). Conflicting findings may be related to a number of factors, including duration of heat stress, length of study, temperature and humidity, muscle, and species. In our study, Angus cattle may have experienced heat stress during the day and milder conditions during the night; these repeated exposures to daily heat stress would have provided some time for cellular adaptations to heat stress. This may also explain why temperature did not influence mt function in Angus. Yet, even if Angus LL is adapting to heat stress, the coupling efficiency and P_{CI+II} remain lower than in Brahman LL.

Overall, temperature had little impact on mt parameters regardless of breed, indicating that 40 °C may be within the optimal range for activity of mt ETS complexes. However, elevated temperature in vivo or *postmortem* muscle may alter metabolism in other ways. In humans, elevated muscle temperature has been shown to increase anaerobic ATP turnover, which may be attributed to higher myosin ATPase and creatine kinase activity (Gray et al., 2011). Similarly, in *postmortem* muscle, higher temperatures are linked to faster ATP turnover and pH decline (Marsh, 1954). Thus, mt may be an important means of generating ATP that would help protect *postmortem* energy status. In fact, mt in Brahman LL would potentially have greater capacity to buffer ATP levels (because of greater P_{CI+II}). Potentially, greater oxygen supply (Mb) could also facilitate higher ATP production; however, we found that Mb expression was similar between breeds. Nonetheless, greater OXPHOS capacity in Brahman LL is consistent with slower pH decline compared to Angus LL during the first 3-h *postmortem* (Wright et al., 2018) and may also explain greater ATP content 1-h *postmortem* (Ramos et al., 2020). Similarly, inhibiting mt function in an in vitro model of *postmortem* metabolism accelerated ATP depletion (Scheffler et al., 2015); and treatments or conditions linked to accelerated energy utilization would utilize ATP and oxygen more quickly, as was shown in the case of electrical stimulation (England et al., 2018).

It is possible that our mt function data reflect changes in mt that occurred within the first hour *postmortem*. Yet, it is important to note that mt in our study were well-coupled and intact, as evidenced by low cyt *c* response; and that our approach of using permeabilized muscle fibers allowed for assessment of all mt kept in situ, regardless of functional status. We concluded that the mt in our samples did not seem to have been damaged during the first hour following slaughter, and that damaged mt were not artificially eliminated by an organelle-isolation protocol. Nevertheless, differences between living and postmortem muscle mt metabolism seem conceivable. However, in permeabilized fibers of porcine LL, ADP-stimulated respiration (with complex I or complex II substrates) at 10 min postmortem is similar to 24 h before slaughter, even though muscle pH has declined to near 6.4 early postmortem (Werner et al., 2010). In addition, the variation in metabolism of a living muscle can be significant depending on activity-related energy demand, such as exercise. The pH of bovine LL at 1-h *postmortem* is generally not less than 6.5, which can be encountered in exercising muscles in humans and rats (Sahlin et al., 1976; Meyer et al., 1986). In our study, muscle properties at 1-h *postmortem* were likely within ranges encountered in working and resting muscle, which leads us to suggest that mt functional parameters were not largely affected within the first hour *postmortem*. However, it does not eliminate the possibility that OXPHOS and coupling efficiency differences between breeds were due to *postmortem* factors, which warrant further investigation.

Greater P_{CI+II} and mt coupling efficiency, along with evidence for slower pH decline in Brahman, could be associated with prolonged maintenance of mt function or integrity; but further investigations are necessary to test this notion. Calcium may play a central role in changes in mt function and integrity that occur during the conversion of muscle to meat. Relatively low levels of calcium in the mt matrix stimulate activity of tricarboxylic acid cycle enzymes (McCormack and Denton, 1989). However, imbalances between ATP production and consumption lead to elevated cytosolic calcium, and subsequently, mt calcium overload. The primary mechanism of mt permeability transition pore opening is calcium overload in the mt matrix (Haworth and Hunter, 1979). Pore opening releases cyt *c*, which results in loss of OXPHOS capacity and mt swelling, and may lead to reverse operation by the mt ATPase. Other factors, including fragmented mt morphology and reactive oxygen species, also contribute to pore opening (reviewed by Hurst et al., 2017). To further complicate matters, mt properties, including resistance to apoptosis and specialization for energy production or calcium homeostasis, vary with fiber type and subcellular location (Picard et al., 2008; Bleck et al., 2018). It is also interesting to point out that inhibition of calcium uptake to the mt matrix accelerates calpain activation and tenderization (Dang et al., 2020). Mitochondria could be a contributing factor to delayed calpain-mediated proteolysis and tenderization that is often observed in Brahman. Thus, there may be more nuanced and yet unknown mechanisms that modulate muscle function and metabolism in these cattle subspecies, which, in turn, could greatly affect the muscle to meat conversion process. Regardless, the distinct phenotypes we observed in our study point to metabolic adaptations in muscle that, in turn, manifest in early *postmortem* metabolism.

Conclusions

After 1-h *postmortem*, mt in LL of Angus and Brahman were capable of OXPHOS and well-coupled. Mitochondrial OXPHOS capacity (P_{CI+II}) and CS activity were higher in Brahman; however, expression of CS and several other mt proteins did not differ between breeds. Thus, mt content does not explain greater OXPHOS capacity in Brahman. Alternatively, OXPHOS capacity and coupling efficiency may be metabolic adaptations related to heat tolerance. Coupling control ratio revealed greater efficiency in Brahman compared to Angus LL, independent of temperature. Taken together, greater OXPHOS capacity, higher CS activity, and greater coupling efficiency in Brahman compared to Angus are evidence of metabolic adaptations in skeletal muscle that could ultimately impact *postmortem* metabolism.

Acknowledgments

This study was financed in part by the Coordenação de Aperfeiçoamento de Pessoal de Nível Superior - Brasil (CAPES) - Finance Code 001 (scholarship for P.M.R.), and by the Agriculture and Food Research Initiative (grant no. 2017-67017-26468) from the USDA National Institute of Food and Agriculture.

Conflict of interest statement

The authors declare no real or perceived conflicts of interest.

Literature Cited

Apaoblaza, A., S. D. Gerrard, S. K. Matarneh, J. C. Wicks, L. Kirkpatrick, E. M. England, T. L. Scheffler, S. K. Duckett, H. Shi, S. L. Silva, *et al.* 2020. Muscle from grass- and grain-fed cattle differs energetically. *Meat Sci.* **161**:107996. doi:10.1016/j.meatsci.2019.107996

Balogh, G., G. Maulucci, I. Gombos, I. Horváth, Z. Török, M. Péter, E. Fodor, T. Páli, S. Benko, T. Parasassi, *et al.* 2011. Heat stress causes spatially-distinct membrane re-modelling in K562 leukemia cells. *PLoS One* **6**:e21182. doi:10.1371/journal.pone.0021182

Beatty, D. T., A. Barnes, E. Taylor, D. Pethick, M. McCarthy, and S. K. Maloney. 2006. Physiological responses of *Bos taurus* and *Bos indicus* cattle to prolonged, continuous heat and humidity. *J. Anim. Sci.* **84**:972–985. doi:10.2527/2006.844972x

Bleck, C. K. E., Y. Kim, T. B. Willingham, and B. Glancy. 2018. Subcellular connectomic analyses of energy networks in striated muscle. *Nat. Commun.* **9**:5111. doi:10.1038/s41467-018-07676-y

Brownstein, A. J., S. Ganesan, C. M. Summers, S. Pearce, B. J. Hale, J. W. Ross, N. Gabler, J. T. Seibert, R. P. Rhoads, L. H. Baumgard, *et al.* 2017. Heat stress causes dysfunctional autophagy in oxidative skeletal muscle. *Physiol. Rep.* **5**:1–13. doi:10.14814/phy2.13317

Connolly, N. M. C., P. Theurey, V. Adam-Vizi, N. G. Bazan, P. Bernardi, J. P. Bolaños, C. Culmsee, V. L. Dawson, M. Deshmukh, M. R. Duchen, *et al.* 2018. Guidelines on experimental methods to assess mitochondrial dysfunction in cellular models of neurodegenerative diseases. *Cell Death Differ.* **25**:542–572. doi:10.1038/s41418-017-0020-4

Dang, D. S., J. F. Buhler, H. T. Davis, K. J. Thornton, T. L. Scheffler, and S. K. Matarneh. 2020. Inhibition of mitochondrial calcium uniporter enhances postmortem proteolysis and tenderness in beef cattle. *Meat Sci.* **162**:108039. doi:10.1016/j.meatsci.2019.108039

Dikmen, S., R. G. Mateescu, M. A. Elzo, and P. J. Hansen. 2018. Determination of the optimum contribution of Brahman genetics in an Angus-Brahman multibreed herd for regulation of body temperature during hot weather. *J. Anim. Sci.* **96**:2175–2183. doi:10.1093/jas/sky133

Divakaruni, A. S., and M. D. Brand. 2011. The regulation and physiology of mitochondrial proton leak. *Physiology* **26**:192–205. doi:10.1152/physiol.00046.2010

Egan, B., and J. R. Zierath. 2013. Exercise metabolism and the molecular regulation of skeletal muscle adaptation. *Cell Metab.* **17**:162–184. doi:10.1016/j.cmet.2012.12.012

Elzo, M. A., D. D. Johnson, J. G. Wasdin, and J. D. Driver. 2012. Carcass and meat palatability breed differences and heterosis effects in an Angus-Brahman multibreed population. *Meat Sci.* **90**:87–92. doi:10.1016/j.meatsci.2011.06.010

England, E. M., S. K. Matarneh, R. M. Mitacek, A. Abraham, R. Ramanathan, J. C. Wicks, H. Shi, T. L. Scheffler, E. M. Oliver, E. T. Helm, *et al.* 2018. Presence of oxygen and mitochondria in skeletal muscle early postmortem. *Meat Sci.* **139**:97–106. doi:10.1016/j.meatsci.2017.12.008

England, E. M., S. K. Matarneh, T. L. Scheffler, C. Wachet, and D. E. Gerrard. 2014. pH inactivation of phosphofructokinase arrests postmortem glycolysis. *Meat Sci.* **98**:850–857. doi:10.1016/j.meatsci.2014.07.019

Fasching, M., M. Fontana-Ayoub, and E. Gnaiger. 2016. Oroboros O2k-protocols chemicals: mitochondrial respiration medium-MiR06, version 06. *Mitochondr. Physiol. Netw.* **14.13**:1–4 [Accessed May 1, 2017]. www.oroboros.at.

Fritzen, A., F. Thøgersen, K. Thybo, C. Vissing, T. Krag, C. Ruiz-Ruiz, L. Risom, F. Wibrand, L. Høeg, B. Kiens, *et al.* 2019. Adaptations in mitochondrial enzymatic activity occurs independent of genomic dosage in response to aerobic exercise training and deconditioning in human skeletal muscle. *Cells* **8**:237. doi:10.3390/cells8030237

Granlund, A., M. Jensen-Waern, and B. Essén-Gustavsson. 2011. The influence of the PRKAG3 mutation on glycogen, enzyme activities and fibre types in different skeletal muscles of exercise trained pigs. *Acta Vet. Scand.* **53**:20. doi:10.1186/1751-0147-53-20

Gray, S. R., K. Soderlund, M. Watson, and R. A. Ferguson. 2011. Skeletal muscle ATP turnover and single fibre ATP and PCr content during intense exercise at different muscle temperatures in humans. *Pflugers Arch.* **462**:885–893. doi:10.1007/s00424-011-1032-4

Hafen, P. S., C. N. Preece, J. R. Sorensen, C. R. Hancock, and R. D. Hyldahl. 2018. Repeated exposure to heat stress induces mitochondrial adaptation in human skeletal muscle. *J. Appl. Physiol.* **125**:1447–1455. doi:10.1152/japplphysiol.00383.2018

Haworth, R. A., and D. R. Hunter. 1979. The Ca^{2+}-induced membrane transition in mitochondria. II. Nature of the Ca^{2+} trigger site. *Arch. Biochem. Biophys.* **195**:460–467. doi:10.1016/0003-9861(79)90372-2

Heden, T. D., P. D. Neufer, and K. Funai. 2016. Looking beyond structure: membrane phospholipids of skeletal muscle mitochondria. *Trends Endocrinol. Metab.* **27**:553–562. doi:10.1016/j.tem.2016.05.007

Hurst, S., J. Hoek, and S. S. Sheu. 2017. Mitochondrial Ca^{2+} and regulation of the permeability transition pore. *J. Bioenerg. Biomembr.* **49**:27–47. doi:10.1007/s10863-016-9672-x

James, R. S., and J. Tallis. 2019. The likely effects of thermal climate change on vertebrate skeletal muscle mechanics with possible consequences for animal movement and behaviour. *Conserv. Physiol.* **7**:1–13. doi:10.1093/conphys/coz066/5610350

Jeremiah, L. E., A. H. Martin, and A. C. Murray. 1985. The effects of various post-mortem treatments on certain physical and sensory properties of three different bovine muscles. *Meat Sci.* **12**:155–176. doi:10.1016/0309-1740(85)90015-4

Kuznetsov, A. V., V. Veksler, F. N. Gellerich, V. Saks, R. Margreiter, and W. S. Kunz. 2008. Analysis of mitochondrial function in situ in permeabilized muscle fibers, tissues and cells. *Nat. Protoc.* **3**:965–976. doi:10.1038/nprot.2008.61

Larsen, S., J. Nielsen, C. N. Hansen, L. B. Nielsen, F. Wibrand, N. Stride, H. D. Schroder, R. Boushel, J. W. Helge, F. Dela, *et al.* 2012. Biomarkers of mitochondrial content in skeletal muscle of healthy young human subjects. *J. Physiol.* **590**:3349–3360. doi:10.1113/jphysiol.2012.230185

Li, C., S. H. White, L. K. Warren, and S. E. Wohlgemuth. 2016. Effects of aging on mitochondrial function in skeletal muscle of American American Quarter Horses. *J. Appl. Physiol.* **121**:299–311. doi:10.1152/japplphysiol.01077.2015

Liu, X., N. Trakooljul, E. Muráni, C. Krischek, K. Schellander, M. Wicke, K. Wimmers, and S. Ponsuksili. 2016. Molecular changes in mitochondrial respiratory activity and metabolic enzyme activity in muscle of four pig breeds with distinct metabolic types. *J. Bioenerg. Biomembr.* **48**:55–65. doi:10.1007/s10863-015-9639-3

Lundby, A. K. M., R. A. Jacobs, S. Gehrig, J. de Leur, M. Hauser, T. C. Bonne, D. Flück, S. Dandanell, N. Kirk, A. Kaech, *et al.* 2018. Exercise training increases skeletal muscle mitochondrial volume density by enlargement of existing mitochondria and not de novo biogenesis. *Acta Physiol.* **222**:1–14. doi:10.1111/apha.12905

Marsh, B. B. 1954. Effects of early post-mortem pH and temperature on beef tenderness. *J. Sci. Food Agric.* **5**:70–75. doi:10.1002/jsfa.2740050202

Matarneh, S. K., M. Beline, S. de Luz E Silva, H. Shi, and D. E. Gerrard. 2018. Mitochondrial F1-ATPase extends glycolysis and pH decline in an in vitro model. *Meat Sci.* **137**:85–91. doi:10.1016/j.meatsci.2017.11.009

Matarneh, S. K., E. M. England, T. L. Scheffler, C. N. Yen, J. C. Wicks, H. Shi, and D. E. Gerrard. 2017. A mitochondrial protein increases glycolytic flux. *Meat Sci.* **133**:119–125. doi:10.1016/j.meatsci.2017.06.007

McCormack, J. G., and R. M. Denton. 1989. The role of Ca^{2+} ions in the regulation of intramitochondrial metabolism and energy production in the mammalian heart. *J. Mol. Cell. Cardiol.* **89**:121–125. doi:10.1016/0022-2828(88)90256-8

Meyer, R. A., T. R. Brown, B. L. Krilowicz, and M. J. Kushmerick. 1986. Phosphagen and intracellular pH changes during contraction of creatine-depleted rat muscle. *Am. J. Physiol.* **250**:C264–C274. doi:10.1152/ajpcell.1986.250.2.C264

Milani, L., and F. Ghiselli. 2020. Faraway, so close. The comparative method and the potential of non-model animals in mitochondrial research. *Philos. Trans. R. Soc. Lond. B. Biol. Sci.* **375**:20190186. doi:10.1098/rstb.2019.0186

Penefsky, H. S. 1985. Mechanism of inhibition of mitochondrial adenosine triphosphatase by dicyclohexylcarbodiimide and oligomycin: relationship to ATP synthesis. *Proc. Natl. Acad. Sci. USA* **82**:1589–1593. doi:10.1073/pnas.82.6.1589

Picard, M., K. Csukly, M. E. Robillard, R. Godin, A. Ascah, C. Bourcier-Lucas, and Y. Burelle. 2008. Resistance to Ca^{2+}-induced opening of the permeability transition pore differs in mitochondria from glycolytic and oxidative muscles. *Am. J. Physiol. Regul. Integr. Comp. Physiol.* **295**:R659–R668. doi:10.1152/ajpregu.90357.2008

Picard, M., R. T. Hepple, and Y. Burelle. 2012. Mitochondrial functional specialization in glycolytic and oxidative muscle fibers: tailoring the organelle for optimal function. *Am. J. Physiol. Cell Physiol.* **302**:C629–C641. doi:10.1152/ajpcell.00368.2011

Porter, C., N. M. Hurren, M. V. Cotter, N. Bhattarai, P. T. Reidy, E. L. Dillon, W. J. Durham, D. Tuvdendorj, M. Sheffield-Moore, E. Volpi, *et al.* 2015a. Mitochondrial respiratory capacity and coupling control decline with age in human skeletal muscle. *Am. J. Physiol. Endocrinol. Metab.* **309**:E224–E232. doi:10.1152/ajpendo.00125.2015

Porter, C., P. T. Reidy, N. Bhattarai, L. S. Sidossis, and B. B. Rasmussen. 2015b. Resistance exercise training alters mitochondrial function in human skeletal muscle. *Med. Sci. Sports Exerc.* **47**:1922–1931. doi:10.1249/MSS.0000000000000605

Ramos, P. M., S. A. Wright, E. F. Delgado, E. van Santen, D. D. Johnson, J. M. Scheffler, M. A. Elzo, C. C. Carr, and T. L. Scheffler. 2020. Resistance to pH decline and slower calpain-1 autolysis are associated with higher energy availability early postmortem in *Bos taurus indicus* cattle. *Meat Sci.* **159**:107925. doi:10.1016/j.meatsci.2019.107925

Ruas, J. S., E. S. Siqueira-Santos, I. Amigo, E. Rodrigues-Silva, A. J. Kowaltowski, and R. F. Castilho. 2016. Underestimation of the maximal capacity of the mitochondrial electron transport system in oligomycin-treated cells. *PLoS One* **11**:e0150967. doi:10.1371/journal.pone.0150967

Sahlin, K., R. C. Harris, B. Nylind, and E. Hultman. 1976. Lactate content and pH in muscle samples obtained after dynamic exercise. *Pflügers Arch. Eur. J. Physiol.* **367**:143–149. doi:10.1007/BF00585150

Saks, V. A., V. I. Veksler, A. V. Kuznetsov, L. Kay, P. Sikk, T. Tiivel, L. Tranqui, J. Olivares, K. Winkler, F. Wiedemann, *et al.* 1998. Permeabilized cell and skinned fiber techniques in studies of mitochondrial function in vivo. *Mol. Cell. Biochem.* **184**:81–100. doi:10.1023/A:1006834912257

Sarlo Davila, K. M., H. Hamblen, P. J. Hansen, S. Dikmen, P. A. Oltenacu, and R. G. Mateescu. 2019. Genetic parameters for hair characteristics and core body temperature in a multibreed Brahman-Angus herd1. *J. Anim. Sci.* **97**:3246–3252. doi:10.1093/jas/skz188

Scheffler, T. L., S. K. Matarneh, E. M. England, and D. E. Gerrard. 2015. Mitochondria influence postmortem metabolism and pH in an in vitro model. *Meat Sci.* **110**:118–125. doi:10.1016/j.meatsci.2015.07.007

Slimen, I. B., T. Najar, A. Ghram, and M. Abdrrabba. 2016. Heat stress effects on livestock: molecular, cellular and metabolic aspects, a review. *J. Anim. Physiol. Anim. Nutr. (Berl)* **100**:401–412. doi:10.1111/jpn.12379

Stefanyk, L. E., N. Coverdale, B. D. Roy, S. J. Peters, and P. J. LeBlanc. 2010. Skeletal muscle type comparison of subsarcolemmal mitochondrial membrane phospholipid fatty acid composition in rat. *J. Membr. Biol.* **234**:207–215. doi:10.1007/s00232-010-9247-4

Stolowski, G. D., B. E. Baird, R. K. Miller, J. W. Savell, A. R. Sams, J. F. Taylor, J. O. Sanders, and S. B. Smith. 2006. Factors influencing the variation in tenderness of seven major beef muscles from three Angus and Brahman breed crosses. *Meat Sci.* **73**:475–483. doi:10.1016/j.meatsci.2006.01.006

Votion, D. M., E. Gnaiger, H. Lemieux, A. Mouithys-Mickalad, and D. Serteyn. 2012. Physical fitness and mitochondrial respiratory capacity in horse skeletal muscle. *PLoS One* **7**:e34890. doi:10.1371/journal.pone.0034890

Wadley, G. D., and G. K. McConell. 2007. Effect of nitric oxide synthase inhibition on water absorption in rat jejunum. *J. Appl. Physiol.* **102**:314–320. doi:10.1152/japplphysiol.00549.2006

Walsh, B., M. Tonkonogi, K. Söderlund, E. Hultman, V. Saks, and K. Sahlin. 2001. The role of phosphorylcreatine and creatine in the regulation of mitochondrial respiration in human skeletal muscle. *J. Physiol.* **537**:971–978. doi:10.1111/j.1469-7793.2001.00971.x

Werner, C., R. Natter, K. Schellander, and M. Wicke. 2010. Mitochondrial respiratory activity in porcine longissimus muscle fibers of different pig genetics in relation to their meat quality. *Meat Sci.* **85**:127–133. doi:10.1016/j.meatsci.2009.12.016

Wright, S. A., P. Ramos, D. D. Johnson, J. M. Scheffler, M. A. Elzo, R. G. Mateescu, A. L. Bass, C. C. Carr, and T. L. Scheffler. 2018. Brahman genetics influence muscle fiber properties, protein degradation, and tenderness in an Angus-Brahman multibreed herd. *Meat Sci.* **135**:84–93. doi:10.1016/j.meatsci.2017.09.006